Effects of magnetic shear on magneto-Rayleigh-Taylor instability

Peng Zhang,[1] Y. Y. Lau,[1,a)] I. M. Rittersdorf,[1] M. R. Weis,[1] R. M. Gilgenbach,[1] D. Chalenski,[1] and S. A. Slutz[2]
[1]*Department of Nuclear Engineering and Radiological Sciences, University of Michigan, Ann Arbor, Michigan 48109-2104, USA*
[2]*Sandia National Laboratories, Albuquerque, New Mexico 87185, USA*

(Received 25 October 2011; accepted 23 December 2011; published online 7 February 2012)

The magnetized liner inertial fusion concept [S. A. Slutz *et al*., Phys. Plasmas **17**, 056303 (2010)] consists of a cylindrical metal liner enclosing a preheated plasma that is embedded in an axial magnetic field. Because of its diffusion into the liner, the pulsed azimuthal magnetic field may exhibit a strong magnetic shear within the liner, offering the interesting possibility of shear stabilization of the magneto-Rayleigh-Taylor (MRT) instability. Here, we use the ideal MHD model to study this effect of magnetic shear in a finite slab. It is found that magnetic shear reduces the MRT growth rate in general. The feedthrough factor is virtually independent of magnetic shear. In the limit of infinite magnetic shear, all MRT modes are stable if $b_u > 1$, where b_u is the ratio of the perturbed magnetic tension in the liner's interior region to the acceleration during implosion.
 [doi:10.1063/1.3680646]

I. INTRODUCTION

Recently, there has been a resurgence of interest in magnetic target fusion.[1] The magnetized liner inertial fusion concept, recently proposed at Sandia National Laboratories,[2] utilizes magnetic compression of a cylindrical, metal liner to adiabatically compress a laser-generated plasma. This plasma is preheated and is embedded in an axial magnetic field. The primary concern in this concept is the magneto-Rayleigh-Taylor (MRT) instability of the liner that could disrupt the symmetry of the implosion.[3–13] As the axial current increases during its risetime, the azimuthal magnetic field it creates may diffuse into the liner, possibly creating a strong radial dependence of the azimuthal magnetic field within the liner. Together with the pre-existing axial magnetic field, the magnetic field within the liner may exhibit a strong magnetic shear, offering the interesting possibility of shear stabilization of MRT.[14,15] This paper examines this issue.

There is a long history of the study of an imploding liner. The earliest theory most relevant to our study is Harris' seminal paper of 1962,[3] and the latest is Ryutov's theory of magnetic cushion.[11] In between one may find the self-similar solutions of Book and Bernstein,[16,17] Han and Suydam,[18] Cassibry *et al*.,[19] Kleev and Velikovich,[20] and Bud'ko *et al*.[21] Reference may be made to simulations of spherical liners by Parks[22] and Samulyak *et al*.,[23] cylindrical liners by Hammer *et al*.,[24] and the scaling studies by Hussey.[25,26] Liberman *et al*.[27] gave an excellent review of the earlier works in Chapters 5 and 6 of their book. Most recently, the effects of gradient on MRT were studied by Yang *et al*. for a particular exponential profile in density and magnetic field.[28] Sinars *et al*. performed a series of controlled experiments of MRT on solid metal liners using the 26-MA Z facility.[8,9] We have ongoing experiments[12,13] exploring MRT growth on planar foils, driven by a 1-MA Linear Transformer Driver (LTD).

Recently, we analytically studied MRT in a finite slab using the ideal MHD model,[10] addressing the problems of feedthrough[29,30] and anisotropy. The classical MRT results of Taylor,[30] Kruskal and Schwarzschild,[4] Chandrasekhar,[5] and Harris[3] are all readily recovered as limiting cases. Since the dominant effects of magnetic shear may be obtained from an ideal MHD model, we shall continue to use such a model to study the effects of magnetic shear on an imploding liner, using a planar geometry as a further simplification. Moreover, we assume that the acceleration is constant and uniform in the unperturbed state, that the plasma is incompressible, and that the subtle difference between cylindrical and planar liner is ignored. In particular, the effects of radial convergence (the Bell-Plesset effects[31–36]) are neglected in the planar geometry. Another crucial assumption is that we ignore the process of magnetic diffusion into the liner. We simply assume that the equivalent azimuthal field varies in a prescribed manner within the liner, from zero magnetic shear to infinite magnetic shear. These two limiting cases can actually be solved analytically in closed form for the sharp boundary model. For intermediate magnetic shear, the MRT eigenmodes need to be solved from a numerical integration of a second order ordinary differential equation. Regardless of the radial dependence of the azimuthal magnetic field, we assume that there is equilibrium in the Cartesian analog. That is, the plasma pressure is adjusted, so that every fluid element undergoes constant acceleration in the lab frame in the unperturbed state.

Section II describes the finite slab model, including the effects of magnetic shear. The results from the model are presented in Sec. III. Concluding remarks are given in Sec. IV.

II. THE MODEL

The model under study is shown in Fig. 1. It consists of three regions, I, II, and III. In the accelerated frame, the three regions are stationary. In this *rest frame of the interfaces*, we

a)Electronic mail: yylau@umich.edu.

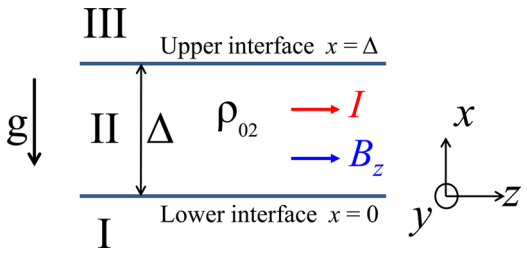

FIG. 1. (Color online) MRT model with two interfaces at $x=0$ and at $x=\Delta$. This paper concentrates on the case where Regions I and III have a negligible mass density compared with Region II.

use the ideal MHD model. In each region, we assume that the fluid is incompressible and is perfectly conducting. Thus, we solve the equations: $\rho(\partial/\partial t+\vec{v}\cdot\nabla)\vec{v}=-\nabla p+\vec{J}\times\vec{B}-\rho g\hat{x}$, $\partial\rho/\partial t+\nabla\cdot(\rho\vec{v})=0$, $\nabla\cdot\vec{v}=0$, $\partial\vec{B}/\partial t=\nabla\times(\vec{v}\times\vec{B})$, and $\nabla\times\vec{B}=\mu_0\vec{J}$. Here, ρ is the mass density, $\vec{v}$ is the fluid velocity, p is the fluid pressure which is assumed to be isotropic, $\vec{J}$ is the current density, $\vec{B}$ is the magnetic field, g is a constant representing the gravity in the negative x-direction [Fig. 1], $\hat{x}$ is the unit vector, and μ_0 is the free space permeability.

For simplicity, we assume region II has a constant density ρ_{02}, and Regions I and III have a negligible density compared with ρ_{02} (i.e., $\rho_{01}\to 0, \rho_{03}\to 0$). Hereafter, all unperturbed quantities are designated with a subscript "0." In equilibrium, the magnetic field, $(0, B_{0y}, B_{0z})$, within each region of Fig. 1 is assumed to be,

$$B_{0z}=\text{constant}, \quad -\infty<x<\infty \text{ (All Regions)}, \tag{1}$$

$$B_{0y}(x)=\begin{cases} B_{01y}=\text{constant}, & x<0 \text{ (Region I)} \quad (2a)\\ B_{02y}(x)=B_{01y}\times\dfrac{\sinh[(1-x/\Delta)/\delta]}{\sinh(1/\delta)}, & 0<x<\Delta \text{ (Region II)}, \quad (2b)\\ B_{03y}=0, & x>\Delta \text{ (Region III)} \quad (2c)\end{cases}$$

where $B_{02y}(x)$ in region II is plotted in Fig. 2. If Fig. 1 is to model the cylindrical geometry, Region II represents the cylindrical liner of thickness Δ, Region I represents the region exterior to the cylindrical liner, and Region III represents the region interior to the cylindrical liner, y represents the azimuthal direction, and $-x$ represents the radial direction. In Eq. (1), B_{0z} represents the pre-existing axial magnetic field. Equation (2) represents the azimuthal magnetic field produced by the axial current on the liner; Eq. (2a) represents the azimuthal magnetic field exterior to the cylindrical liner, Eq. (2c) represents the azimuthal magnetic field interior to the cylindrical liner (which is zero), and Eq. (2b) represents the diffusion of the azimuthal magnetic field into the liner. The x-dependence in Eq. (2b) signifies the magnetic shear, measured by the dimensionless parameter δ (Fig. 2). A small δ means that the azimuthal magnetic field barely diffuses into the liner, corresponding to strong magnetic shear. The infinite δ limit corresponds to a constant magnetic shear within the liner, i.e., $dB_{0y}/dx=-B_{01y}/\Delta=$ constant, as shown in Fig. 2 and Eq. (2b). Thus, δ in some sense is analogous to the "skin depth," in units of the liner thickness Δ (Fig. 2). Also shown in Fig. 2 is the case of zero magnetic shear, i.e., the azimuthal magnetic field penetrates the entire liner. This case is included for completeness, as it has a closed form solution[10,13] and it sets the bounds of MRT growth from zero to infinite magnetic shear (see Fig. 4).

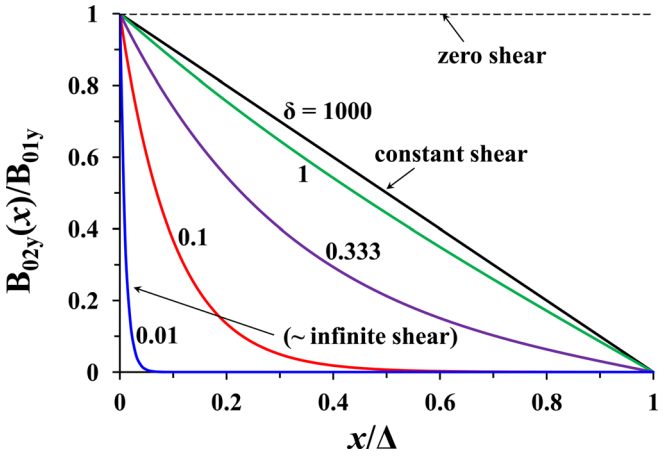

FIG. 2. (Color online) The profile of the y component of magnetic field $B_{02y}(x)$ in Region II, $0<x<\Delta$, at various δ, indicating different degree of magnetic shear.

We consider a small signal perturbation on the equilibrium of the 3-region geometry shown in Fig. 1, with the defined magnetic field profile in Eqs. (1) and (2). Within each region, I, II, or III, all perturbation quantities are assumed to be of the form $u_1(x)e^{i\omega t-ik_y y-ik_z z}$. The ideal MHD equations are linearized to obtain the eigenvalue equation[14] as

$$\frac{d}{dx}\left\{\left[\rho_0(-\omega^2)+\frac{1}{\mu_0}\left(\vec{k}\cdot\vec{B}_0\right)^2\right]\frac{d\xi_{1x}}{dx}\right\} - k^2\left[\rho_0(-\omega^2)-g\frac{d\rho_0}{dx}+\frac{1}{\mu_0}\left(\vec{k}\cdot\vec{B}_0\right)^2\right]\xi_{1x}=0, \quad -\infty<x<\infty, \tag{3}$$

where $\vec{B}_0=\hat{y}B_{0y}(x)+\hat{z}B_{0z}(x)$, $\vec{k}=\hat{y}k_y+\hat{z}k_z$, $k=\sqrt{k_y^2+k_z^2}$, and ξ_{1x} is the perturbation displacement in the x-direction. Note that Eq. (3) is valid for general density profile $\rho_0(x)$ and for general magnetic field profiles $B_{0y}(x)$ and $B_{0z}(x)$. The eigenvalue, ω^2, and the corresponding eigenfunction, $\xi_{1x}(x)$, need to be solved numerically from Eq. (3). It is easy to show from Eq. (3) that ω^2 is always real.[5,14] The MRT growth rate is given by $\gamma=-\text{Im}(\omega)$. The feedthrough factor for the unstable mode, from the lower interface to the upper interface, is obtained from its eigenfunction, $|\xi_{1x}(x=\Delta)/\xi_{1x}(x=0)|$. (In Fig. 1, since Region II has the

highest density, it is clear that the lower interface ($x=0$) is RT-unstable, whereas the upper interface ($x=\Delta$) is RT-stable. How the ripples on the unstable interface transmit to the stable interface is known as "feedthrough"[29] and is primarily determined by the ratio of the unstable mode's eigenfunction at the edges of the finite slab.[10,29,30])

If the density profile $\rho_0(x)$ has a jump discontinuity, as shown in Fig. 1, the direct numerical integration of Eq. (3) is not straightforward. Instead, we analytically solved for the solutions in Regions I and III and used these solutions as the boundary conditions for the numerical solution in Region II. The details are given in the Appendix. In Region II, $0 < x < \Delta$, the eigenvalue equation Eq. (3) reads [cf. Eq. (A7)],

$$\frac{d}{d\bar{x}}\left\{[\bar{\gamma}^2 + b_2^2(\bar{x})]\frac{d\xi_{1x}}{d\bar{x}}\right\} - [\bar{\gamma}^2 + b_2^2(\bar{x})]\xi_{1x} = 0. \tag{4}$$

The boundary conditions to Eq. (4) are [cf. Eqs. (A5a) and (A5b)]

$$\left.\frac{1}{\xi_{1x}}\frac{d\xi_{1x}}{d\bar{x}}\right|_{\bar{x}=0^+} = \frac{b_l^2 - 1}{\bar{\gamma}^2 + b_l^2}, \tag{5}$$

$$\left.\frac{1}{\xi_{1x}}\frac{d\xi_{1x}}{d\bar{x}}\right|_{\bar{x}=k\Delta^-} = -\frac{b_u^2 + 1}{\bar{\gamma}^2 + b_u^2}, \tag{6}$$

where $\bar{x} = kx$, $\bar{\gamma} = \gamma/\sqrt{kg}$. In Eqs. (4)–(6),

$$b_l^2 = \frac{(\vec{k}\cdot\vec{B}_0)_{\rm I}^2}{\mu_0\rho_{02}(kg)}, \quad b_2^2 = \frac{(\vec{k}\cdot\vec{B}_0)_{\rm II}^2}{\mu_0\rho_{02}(kg)}, \quad b_u^2 = \frac{(\vec{k}\cdot\vec{B}_0)_{\rm III}^2}{\mu_0\rho_{02}(kg)}, \tag{7}$$

$$b_2(\bar{x}) = b_u + (b_l - b_u)\frac{\sinh[(1-\bar{x}/k\Delta)/\delta]}{\sinh(1/\delta)}. \tag{8}$$

Note that the magnetic field effects in the three regions, I, II, III, enter through the normalized magnetic tension, b_ℓ^2, b_2^2 and b_u^2, respectively. The magnetic shear effect enters through δ in $b_2(\bar{x})$, given in Eq. (8). Equations (4)–(6) may then be solved numerically once b_ℓ, b_u, and δ are specified.

As a check, let us consider the special case where there is no magnetic tension in Regions I and III, i.e., $b_\ell = b_u = 0$. The MRT in this case was shown by Harris[3] to be identical to the classical Rayleigh-Taylor instability on a finite slab that was treated by Taylor.[29,30] For this case, we have $b_2 = 0$ for all x. An eigenfunction to Eq. (4) is clearly $\xi_{1x}(\bar{x}) = e^{-\bar{x}}$, whose eigenvalue is $\bar{\gamma}^2 = 1$, as is obvious from either Eq. (5) or (6). This eigenvalue corresponds to the familiar MRT dispersion relation for the unstable mode, $\omega^2 = -kg$, whose feedthrough factor is $e^{-k\Delta}$. The other eigenfunction to Eq. (4) is $\xi_{1x}(\bar{x}) = e^{\bar{x}}$, whose eigenvalue is $\bar{\gamma}^2 = -1$, as is also readily obtained from either Eq. (5) or Eq. (6). This eigenvalue corresponds to the stable modes in the R-T dispersion relation, $\omega^2 = kg$, whose feedthrough factor is $e^{k\Delta}$. These results are consistent with Taylor and Harris.[10]

In the limits of zero and of infinite magnetic shear, the magnetic field within Region II is a constant, whose normalized magnetic tension is designated by b_2^2. In terms of b_ℓ^2, b_2^2, and b_u^2, the normalized eigenfrequency, $\bar{\omega} = \omega/\sqrt{kg}$, is governed by the 4th degree polynomial, $\bar{\omega}^4 - \bar{R}\bar{\omega}^2 + \bar{S} = 0$, where

$$\bar{R} = 2b_2^2 + (b_u^2 + b_\ell^2)\coth k\Delta,$$
$$\bar{S} = b_2^4 - 1 + b_\ell^2(b_2^2\coth k\Delta + b_u^2 + 1) + b_u^2(b_2^2\coth k\Delta - 1). \tag{9a,b}$$

The unstable MRT mode exists if and only if $\bar{S} < 0$. It then follows from Eq. (9b) that the most dangerous MRT mode is the one with $b_\ell = 0$, or equivalently, $(\vec{k}\cdot\vec{B}_0)_{\rm I} = 0$. The mode that does not bend the magnetic field line on the lower interface is the most difficult to stabilize.[5,6,10,14] It is of interest to note that this most dangerous mode, with $b_\ell = 0$ or $(\vec{k}\cdot\vec{B}_0)_{\rm I} = 0$, corresponds to waves which travel perpendicular to the magnetic field, a property shared by purely magnetosonic waves. In the numerical results presented in Sec. III, we, therefore, concentrate on this case.

In Eqs. (9a) and (9b), the zero magnetic shear case corresponds to $b_2 = b_\ell$ since $B_{02y}(x) = B_{01y} =$ constant in Eq. (2). In this case, the $b_\ell = 0$ is always unstable regardless of the axial magnetic field B_{0z}, and the normalized growth rate for this zero magnetic shear case is given by

$$\bar{\gamma}^2 = \frac{\sqrt{b_u^4\coth^2(k\Delta) + 4(1+b_u^2)} - b_u^2\coth(k\Delta)}{2}. \tag{10}$$

Equation (10) is easily derived from Eqs. (9a,b), where $\bar{R} = b_u^2\coth k\Delta$, $\bar{S} = -1 - b_u^2$. Equation (10) is also plotted in Figs. 3 and 4 as dotted curves. The infinite magnetic shear case corresponds to $b_2 = b_u$ (Fig. 2), in which case the $b_\ell = 0$ mode (and therefore *all* MRT modes) are stabilized if $b_u \geq 1$.

III. RESULTS

In this section, we shall concentrate mainly on the most dangerous MRT mode with $b_\ell = 0$, i.e., $(\vec{k}\cdot\vec{B}_0)_{\rm I} = 0$, as explained toward the end of Sec. II. Figure 3 shows the normalized MRT growth rate, $\bar{\gamma} = -{\rm Im}(\omega_1)/\sqrt{kg}$, for this $b_\ell = 0$ case, as a function of $k\Delta$. Various combinations of magnetic field tension in Region III, b_u, and of the magnetic shear (δ) are presented. These results were obtained from the numerical solutions to Eqs. (4)–(6). For a given δ, the MRT growth rate decreases as b_u increases (Fig. 3). As the magnetic shear increases, i.e., as δ decreases from Fig. 3(a) to Fig. 3(d), the MRT growth rate decreases in general, demonstrating the stabilizing influence of magnetic shear. However, the MRT growth rate cannot be completely eliminated by magnetic shear, even when δ is close to zero (but not equal to zero), as shown in Fig. 3(d).

Figure 4 shows the effect of magnetic shear (δ) for the specific case of $b_\ell = 0$, $b_u = 1$. It is clear that increasing magnetic shear reduces the MRT growth rate. However, the MRT growth rate remains significant, about 40 percent of $(kg)^{1/2}$ even when $\delta = 0.01$ (Fig. 4). If $\delta = 0$ (infinite magnetic shear), all MRT modes are stabilized if $b_u \geq 1$. This is consistent with the numerical calculation of Eqs. (4)–(6), as shown in Figs. 3 and 4.

For the most dangerous mode, $b_\ell = 0$, there is the relationship $|k_y/k_z| = |B_{0z}/B_{01y}|$, from which it is easy to show that $b_u^2 = 2k\Delta/(1 + B_{01y}^2/B_{0z}^2) = 2k_z\Delta/[(B_{01y}/B_{0z})(1 + B_{01y}^2/$

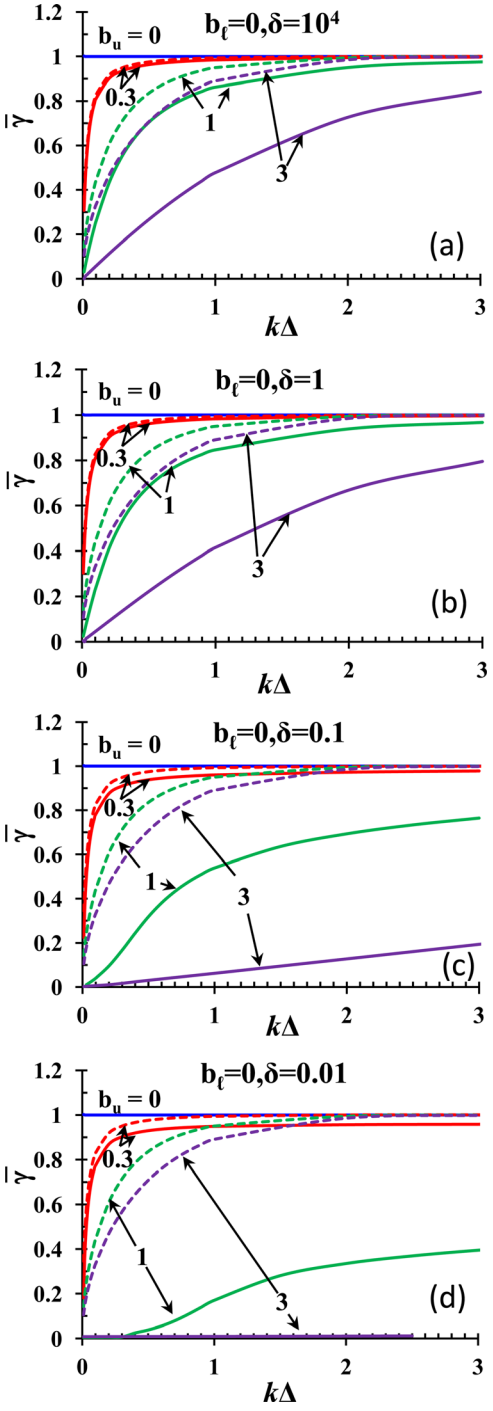

FIG. 3. (Color online) The normalized MRT growth rate for the $b_\ell = 0$ case, as a function of $k\Delta$, at various b_u, for (a) $\delta = 10^4$, (b) $\delta = 1$, (c) $\delta = 0.1$, (d) $\delta = 0.01$. The solid lines show the numerical solutions from Eqs. (4)–(6), the dotted lines show the analytical results of Eq. (10), i.e., the zero magnetic shear case.

$B_{0z}^2)^{1/2}]$ upon using the equilibrium condition $\rho_{02}\Delta g = B_{01y}^2/2\mu_0$ for the configuration of Fig. 1. We may then re-plot Fig. 3 to show the normalized MRT growth rate $\bar{\gamma}$ as a function of $k_z\Delta$ at a fixed value of B_{01y}^2/B_{0z}^2. Figure 5 shows such graphs with $B_{01y}^2/B_{0z}^2 = 0.1$, 1.0, and 10. These graphs show the effect of magnetic shear (δ) on the most unstable mode, $b_\ell = 0$. If the magnetic shear is small or moderate, e.g., $\delta = 10^4$ and $\delta = 1$ in Fig. 5, the normalized MRT growth rate increases as a function of $k_z\Delta$. If the magnetic shear is large,

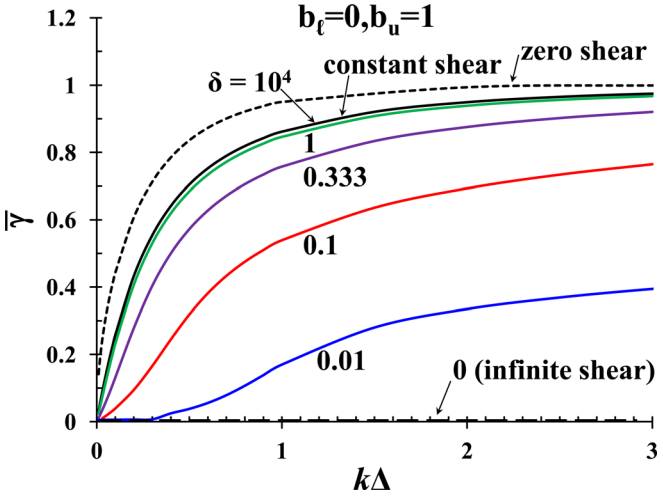

FIG. 4. (Color online) The normalized MRT growth rate for the case of $b_\ell = 0$ and $b_u = 1$, as a function of $k\Delta$, at various δ. The solid lines are from Eqs. (4)–(6), the dotted line is from Eq. (10), i.e., the zero magnetic shear case, and the dashed line indicates the infinite shear case ($\delta = 0$), where MRT does not exist if $b_u \geq 1$.

e.g., $\delta = 0.1$ and $\delta = 0.01$ in Fig. 5, the growth rate decreases as $k_z\Delta$ increases. For infinite magnetic shear, $\bar{\gamma} = 0$ for $b_u \geq 1$, as shown in Figs. 5(a) and 5(b). At a given value of δ, as the magnetic field ratio B_{01y}^2/B_{0z}^2 increases, b_u decreases; thus the MRT growth rate increases, as shown in Fig. 5, which is consistent with the results shown in Figs. 3 and 4.

Figure 5 suggests that an axial magnetic field comparable to the azimuthal magnetic field is needed to suppress MRT growth. A plausible way to generate such a high axial magnetic field is to surround the metallic liner with a thick, low density foam. As this foam is imploded radially, the (initially low) axial magnetic field that is imbedded in it may be compressed to a high value. The MRT growth in such a thick foam (low aspect ratio) may not pose as a serious problem, or one could tailor its density to stabilize the implosion.

The feedthrough factor, equal to the perturbation displacement ratio $|\xi_{1x}(x = \Delta)/\xi_{1x}(x = 0)|$, may also be calculated from Eqs. (4)–(6). Figure 6(a) shows the feedthrough factor for the $b_\ell = 0$, $\delta = 0.1$ case, as a function of $k\Delta$ at various values of b_u. The feedthrough factor is reduced with increasing b_u, in which case the upper interface is less likely to form a ripple because of the magnetic tension there. Thus, the MRT growth at the lower interface is less likely to be transmitted to the upper interface.[10] Figure 6(b) shows that the feedthrough factor is virtually independent of the magnetic shear (δ). This is verified by the asymptotic dependence of the feedthrough factors (dotted lines in Fig. 6), which is derived for the case of no magnetic shear effect, given by Eqs. (11) and (12) of Ref. 10. It is interesting to note that the asymptotic formulas for large $k\Delta$ are already very accurate when $k\Delta > 2$.

IV. CONCLUDING REMARKS

This paper presents a simple, ideal MHD model to study the effects of magnetic shear on MRT in a magnetized liner. While MRT growth may not be completely eliminated even

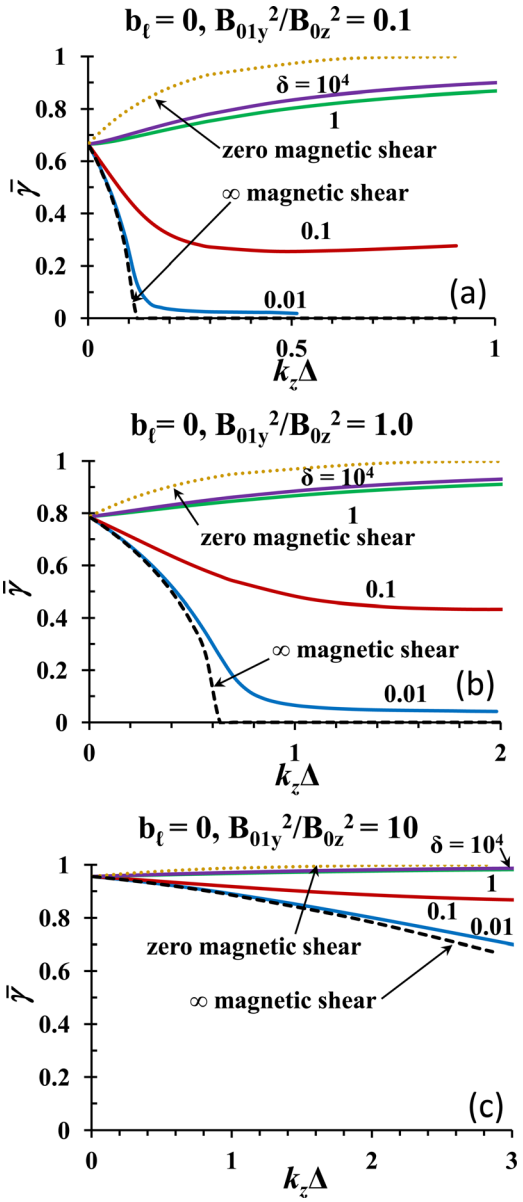

FIG. 5. (Color online) The normalized MRT growth rate versus $k_z\Delta$ for the case of $b_\ell = 0$ and (a) $B_{01y}^2/B_{0z}^2 = 0.1$, (b) $B_{01y}^2/B_{0z}^2 = 1.0$, and (c) $B_{01y}^2/B_{0z}^2 = 10$, at various δ. The solid lines show the numerical solutions from Eqs. (4)–(6), the dotted lines show the analytical results of Eq. (9), for both the zero magnetic shear case [cf. Eq. (10)] and infinite magnetic shear case.

with strong magnetic shear, magnetic shear does reduce the MRT growth rate in general. The feedthrough factor is also computed and is found to be insensitive to the magnetic shear. In the limit of infinite magnetic shear, all MRT modes

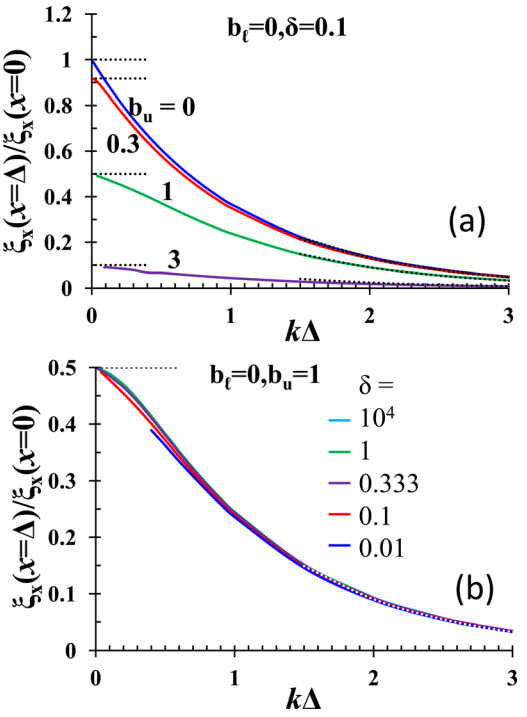

FIG. 6. (Color online) The feedthrough factor as a function of $k\Delta$, for (a) $b_\ell = 0$, $\delta = 0.1$ at various b_u from 0 to 3, (b) $b_\ell = 0$, $b_u = 1$, at various δ from 10^4 to 0.01. The dashed lines are given by Eqs. (11) and (12) of Ref. 10.

are stabilized if $b_u \geq 1$. The full implications of MRT on the magnetized liner inertial fusion concept [2] await further studies.

ACKNOWLEDGMENTS

We acknowledge fruitful discussions with Dan Sinars, Mike Cuneo, Mark Herrmann, Sasha Velikovich, and Dimitri Ryutov. This work was supported by DoE award number DE-SC0002590, NSF grant number PHY 0903340, and by US DoE through Sandia National Labs award numbers 240985 and 76822 to the U of Michigan. Sandia is a multiprogram laboratory operated by Sandia Corporation, a Lockheed Martin Company, for the US DoE's NNSA under Contract DE-AC04-94AL85000.

APPENDIX

From Eq. (3) of the main text, the effects of magnetic field enter through the term $\vec{k}\cdot\vec{B}_0$. For each Region of Fig. 1, this term reads,

$$\begin{cases} (\vec{k}\cdot\vec{B}_0)_{\rm I} = k_y B_{01y} + k_z B_{0z} = \text{constant}, & x < 0 \text{ (Region I)} \\ (\vec{k}\cdot\vec{B}_0)_{\rm II} = k_y B_{01y}\dfrac{\sinh[(1-x/\Delta)/\delta]}{\sinh(1/\delta)} + k_z B_{0z}, & 0 < x < \Delta \text{ (Region II)} \\ (\vec{k}\cdot\vec{B}_0)_{\rm III} = k_z B_{0z} = \text{constant}, & x > \Delta \text{ (Region III)}, \end{cases} \tag{A1}$$

according to Eqs. (1) and (2). Thus, the solution to Eq. (3) in Regions I and III is simply,

$$\xi_{1x} = \xi_{1x}(x=0)e^{kx}, \quad x < 0 \text{ (Region I)}, \tag{A2a}$$

$$\xi_{1x} = \xi_{1x}(x=\Delta)e^{-k(x-\Delta)}, \quad x > \Delta \text{ (Region III)}. \tag{A2b}$$

To solve Eq. (3) in Region II, we first integrate Eq. (3) across the two interfaces, at $x=0$ and $x=\Delta$, respectively, to obtain

$$\left\{\left[\rho_0(x)\gamma^2+\frac{1}{\mu_0}(\vec{k}\cdot\vec{B}_0)^2\right]\frac{d\xi_{1x}}{dx}\right\}\Big|_{x=0^-}^{x=0^+}=-k^2g\rho_{02}\xi_{1x}(x=0), \tag{A3a}$$

$$\left\{\left[\rho_0(x)\gamma^2+\frac{1}{\mu_0}(\vec{k}\cdot\vec{B}_0)^2\right]\frac{d\xi_{1x}}{dx}\right\}\Big|_{x=\Delta^-}^{x=\Delta^+}=+k^2g\rho_{02}\xi_{1x}(x=\Delta), \tag{A3b}$$

where ρ_{02} is the constant mass density of Region II. Upon using Eqs. (A2a) and (A2b) into Eqs. (A3a) and (A3b), we obtain

$$\left[\gamma^2+\frac{1}{\mu_0\rho_{02}}\left(\vec{k}\cdot\vec{B}_0\right)^2\Big|_{x=0^+}\right]\frac{1}{k\xi_{1x}}\frac{d\xi_{1x}}{dx}\Big|_{x=0^+} -\frac{1}{\mu_0\rho_{02}}\left(\vec{k}\cdot\vec{B}_0\right)^2\Big|_{x=0^-}=-kg, \tag{A4a}$$

$$\frac{1}{\mu_0\rho_{02}}\left(\vec{k}\cdot\vec{B}_0\right)^2\Big|_{x=\Delta^+} -\left[\gamma^2+\frac{1}{\mu_0\rho_{02}}\left(\vec{k}\cdot\vec{B}_0\right)^2\Big|_{x=\Delta^-}\right]\frac{1}{k\xi_{1x}}\frac{d\xi_{1x}}{dx}\Big|_{x=\Delta^-}=+kg. \tag{A4b}$$

Assuming that there is no surface current at both interfaces at $x=0$ and $x=\Delta$, as the surface current spreads out to a distance of order the "skin depth" even when that "skin depth" is small, we have $(\vec{k}\cdot\vec{B}_0)^2|_{x=0^+}=(\vec{k}\cdot\vec{B}_0)^2|_{x=0^-}$ and $(\vec{k}\cdot\vec{B}_0)^2|_{x=\Delta^-}=(\vec{k}\cdot\vec{B}_0)^2|_{x=\Delta^+}$for the present model. Equations (A4a) and (A4b) may then be expressed in the normalized form, respectively, as

$$\frac{1}{\xi_{1x}}\frac{d\xi_{1x}}{d\bar{x}}\Big|_{\bar{x}=0^+}=\frac{b_l^2-1}{\bar{\gamma}^2+b_l^2}, \tag{A5a}$$

$$\frac{1}{\xi_{1x}}\frac{d\xi_{1x}}{d\bar{x}}\Big|_{\bar{x}=k\Delta^-}=-\frac{b_u^2+1}{\bar{\gamma}^2+b_u^2}, \tag{A5b}$$

where $\bar{x}=kx$, $\bar{\gamma}=\gamma/\sqrt{kg}$, $b_l^2=\frac{(\vec{k}\cdot\vec{B}_0)_{\rm I}^2}{\mu_0\rho_{02}(kg)}$, $b_u^2=\frac{(\vec{k}\cdot\vec{B}_0)_{\rm III}^2}{\mu_0\rho_{02}(kg)}$. Equations (A5a) and (A5b) are Eqs. (5) and (6) of the main text. From Eq. (A1), it can be easily shown that

$$b_2(\bar{x})=\frac{(\vec{k}\cdot\vec{B}_0)_{\rm II}}{\sqrt{\mu_0\rho_{02}kg}}=b_u+(b_l-b_u)\frac{\sinh[(1-\bar{x}/k\Delta)/\delta]}{\sinh(1/\delta)}, \tag{A6}$$

where we have used Eq. (2b) of the main text. Thus, in Region II, the governing Eq. (3) becomes

$$\frac{d}{d\bar{x}}\left\{[\bar{\gamma}^2+b_2^2(\bar{x})]\frac{d\xi_{1x}}{d\bar{x}}\right\}-[\bar{\gamma}^2+b_2^2(\bar{x})]\xi_{1x}=0,\ 0<x<\Delta, \tag{A7}$$

which is Eq. (4) in the main text.

[1]R. C. Kirtpatrick, I. R. Lindemuth, and M. S. Ward, Fusion Technol. **27**, 201 (1995).
[2]S. A. Slutz, M. C. Herrmann, R. A. Vesey, A. B. Sefkow, D. B. Sinars, D. C. Rovang, K. J. Peterson, and M. E. Cuneo, Phys. Plasmas **17**, 056303 (2010).
[3]E. G. Harris, Phys. Fluids **5**, 1057 (1962).
[4]M. Kruskal and M. Schwarzschild, Proc. R. Soc. (London), **A223**, 348 (1954).
[5]S. Chandrasekhar, *Hydrodynamic and Hydromagnetic Stability* (Oxford University Press, London, UK, 1961), p. 429.
[6]D. D. Ryutov, M. S. Derzon, and M. K. Matzen, Rev. Mod. Phys. **72**, 167 (2000).
[7]D. L. Peterson, R. L. Bowers, W. Matuska, K. D. McLenithan, G. A. Chandler, C. Deeney, M. S. Derzon, M. R. Douglas, M. K. Matzen, T. J. Nash, R. B. Spielman, K. W. Struve, W. A. Stygar, and N. F. Roderick, Phys. Plasmas **6**, 2178 (1999).
[8]D. B. Sinars, S. A. Slutz, M. C. Herrmann, R. D. McBride, M. E. Cuneo, K. J. Peterson, R. A. Vesey, C. Nakhleh, B. E. Blue, K. Killebrew, D. Schroen, K. Tomlinson, A. D. Edens, M. R. Lopez, I. C. Smith, J. Shores, V. Bigman, G. R. Bennett, B. W. Atherton, M. Savage, W. A. Stygar, G. T. Leifeste, and J. L. Porter, Phys. Rev. Lett. **105**, 185001 (2010).
[9]D. B. Sinars, S. A. Slutz, M. C. Herrmann, R. D. McBride, M. E. Cuneo, C. A. Jennings, J. P. Chittenden, A. L. Velikovich, K. J. Peterson, R. A. Vesey, C. Nakhleh, E. M. Waisman, B. E. Blue, K. Killebrew, D. Schroen, K. Tomlinson, A. D. Edens, M. R. Lopez, I. C. Smith, J. Shores, V. Bigman, G. R. Bennett, B. W. Atherton, M. Savage, W. A. Stygar, G. T. Leifeste, and J. L. Porter, Phys. Plasmas **18**, 056301 (2011).
[10]Y. Y. Lau, J. C. Zier, I. M. Rittersdorf, M. R. Weis, and R. M. Gilgenbach, Phys. Rev. E **83**, 006405 (2011).
[11]D. D. Ryutov, Phys. Plasmas **18**, 064509 (2011).
[12]J. C. Zier, Doctoral Dissertation, University of Michigan, Ann Arbor (2010).
[13]Y. Y. Lau, J. C. Zier, I. M. Rittersdorf, M. R. Weis, and R. M. Gilgenbach, in AIP Proceedings of the Dense Z-Pinch, Biarritz, France, 2011.
[14]P. M. Bellan, *Fundamentals of Plasma Physics* (Cambridge University Press, 2006), p. 349.
[15]P. Zhang, Y. Y. Lau, I. M. Rittersdorf, M. R. Weis, R. M. Gilgenbach, S. A. Slutz, D. B. Sinars, M. C. Herrmann, and M. E. Cuneo, *Bull. Am. Phys. Soc*. (APS-DPP, Salt Lake City, Utah, Nov. 2011).
[16]D. L. Book and I. B. Bernstein, Phys. Fluids **22**, 79 (1979).
[17]D. L. Book and I. B. Bernstein, J. Plasma Phys. **23**, 521 (1980).
[18]S. J. Han and B. R. Suydam, Phys. Rev. A **26**, 926 (1982).
[19]J. T. Cassibry, R. J. Cortez, S. C. Hsu, and F. D. Witherspoon, Phys. Plasmas **16**, 112707 (2009).
[20]A. I. Kleev and A. L. Velikovich, Plasma Phys. Controlled Fusion, **32**, 763 (1990).
[21]A. B. Bud'ko, M. A. Liberman, A. L. Velikovich, and F. S. Felber, Phys. Fluids B **1**, 598 (1989).
[22]P. B. Parks, Phys. Plasmas **15**, 062506 (2008).
[23]R. Samulyak, P. Parks, and L. Wu, Phys. Plasmas **17**, 092702 (2010).
[24]J. H. Hammer, J. L. Eddleman, P. T. Springer, M. Tabak, A. Toor, K. L. Wong, G. B. Zimmerman, C. Deeney, R. Humphreys, T. J. Nash, T. W. L. Sanford, R. B. Spielman, and J. S. De Groot, Phys. Plasmas **3**, 2063 (1996).
[25]T. W. Hussey, N. F. Roderick, and D. A. Kloc, J. Appl. Phys. **51**, 1452 (1980).
[26]T. W. Hussey, M. K. Matzen, and N. F. Roderick, J. Appl. Phys. **58**, 2677 (1986).
[27]M. A. Liberman, J. S. De Groot, A. Toor, and R. B. Spielman, *Physics of High-Density Z-Pinch Plasmas* (Springer-Verlag, New York, 1999).
[28]B. L. Yang, L. F. Wang, W. H. Ye, and C. Xue, Phys. Plasmas **18**, 072111 (2011).
[29]S. Atzeni and J. Meyer-Ter-Vehn, *The Physics of Inertial Fusion* (Oxford University Press, New York, 2004), p. 253.
[30]G. I. Taylor, Proc. R. Soc. (London) **A201**, 192 (1950).
[31]G. I. Bell, Los Alamos Scientific Laboratory, Report LA-1321, 1951.
[32]M. S. Plesset, J. Appl. Phys. **25**, 96 (1954).
[33]J. B. Beck, Ph.D. thesis, Purdue University, 1996.
[34]W. Hsing, C. W. Barnes, J. B. Beck, N. M. Hoffman, D. Galmiche, A. Richard, J. Edwards, P. Graham, S. Rothman, and B. Thomas, Phys. Plasmas **4**, 1832 (1997).
[35]V. N. Goncharov, P. W. McKenty, and S. Skupsky, Phys. Plasmas **7**, 5118 (2000).
[36]P. Amendt, J. D. Colvin, J. D. Ramshaw, H. F. Robey, and O. L. Landen, Phys. Plasmas **10**, 820 (2003).